HHS Public Access

Author manuscript

Br J Pharmacol. Author manuscript; available in PMC 2024 October 01.

Published in final edited form as:

Br J Pharmacol. 2023 October ; 180(20): 2623–2640. doi:10.1111/bph.16148.

Complementary roles of EP2 and EP4 receptors in malignant glioma

Jiange Qiu[1,2], **Qianqian Li**[2,3], **Junqi Li**[4], **Fengmei Zhou**[1], **Peng Sang**[1], **Zhongkun Xia**[1], **Wei Wang**[1], **Lin Wang**[1], **Ying Yu**[3], **Jianxiong Jiang**[2,3]

[1]Academy of Medical Science, Zhengzhou University, Zhengzhou, Henan, China

[2]Division of Pharmaceutical Sciences, James L. Winkle College of Pharmacy, University of Cincinnati, Cincinnati, Ohio, USA

[3]Department of Pharmaceutical Sciences, College of Pharmacy, University of Tennessee Health Science Center, Memphis, Tennessee, USA

[4]Medical Research Center, Institute of Neuroscience, the Third Affiliated Hospital, Zhengzhou University, Zhengzhou, China

Abstract

Background and Purpose: Glioblastoma (GBM) is the most aggressive brain tumor in the central nervous system, but the current treatment is very limited and overall unsatisfactory. PGE_2-initiated cAMP signaling via EP2 and EP4 receptors is involved in the tumorigenesis of multiple cancer types. However, whether or how EP2 and EP4 contribute to GBM growth largely remains elusive.

Experimental Approach: We performed comprehensive data analyses of gene expression in human GBM samples and determined their expression correlations through multiple bioinformatics approaches. A time-resolved fluorescence energy transfer (TR-FRET) assay was utilized to characterize the PGE_2-mediated cAMP signaling via EP2 and EP4 receptors in human glioblastoma cells. Taking advantage of potent and selective small-molecule antagonists that were recently reported, we determined the effects of pharmacological inhibition of EP2 or EP4 on GBM growth in both subcutaneous and intracranial tumor models.

Correspondence: Qianqian Li, Department of Pharmaceutical Sciences, College of Pharmacy, University of Tennessee Health Science Center, 881 Madison Avenue, Pharmacy Building, Suite 610, Memphis, TN 38163, USA. qli42@uthsc.edu, Ying Yu, Department of Pharmaceutical Sciences, College of Pharmacy, University of Tennessee Health Science Center, 881 Madison Avenue, Pharmacy Building, Suite 664, Memphis, TN 38163, USA. yyu26@uthsc.edu, Jianxiong Jiang, Department of Pharmaceutical Sciences, College of Pharmacy, University of Tennessee Health Science Center, 881 Madison Avenue, Pharmacy Building, Suite 665, Memphis, TN 38163, USA. jjiang18@uthsc.edu.

Author Contributions

J.Q., Q.L., Y.Y. and J.J. participated in the research design; J.Q., Q.L., J.L., F.Z., P.S., Z.X., W.W., L.W., Y.Y. and J.J. conducted the experiments; J.Q., Q.L., Y.Y. and J.J. performed the data analyses; J.Q., Q.L., Y.Y. and J.J. wrote the manuscript. All authors reviewed and revised the final version of manuscript and approved manuscript submission.

Conflict of Interest

The authors declare no conflicts of interest.

Ethics approval statement:

All animal care and experimental procedures performed in this study were done in accordance with the guide for the Care and Use of Laboratory animals adopted by the US National Institutes of Health and the guidelines of the Institutional Animal Care and Use Committee (IACUC).

Key Results: The expression of both EP2 and EP4 receptors were upregulated and highly correlated with a variety of tumor-promoting cytokines, chemokines, and growth factors in human gliomas. Further, they were heterogeneously expressed in human GBM cells, where they compensated each other to mediate PGE_2-initiated cAMP signaling and to promote colony formation, cell invasion and migration. Pharmacological inhibition of EP2 and EP4 revealed that these two PGE_2 receptors might mediate GBM growth, angiogenesis, and immune evasion in a compensatory manner.

Conclusion and Implications: The compensatory roles of EP2 and EP4 in GBM development and growth suggest that concurrently targeting these two $G\alpha_s$-coupled PGE_2 receptors might represent a more effective strategy than inhibiting either EP2 or EP4 alone for GBM treatment.

Keywords

Antagonist; COX; GBM; Glioblastoma; PD-L1; Prostaglandin; Tumor microenvironment; Tumor inflammation

Introduction

Glioblastoma (GBM) is the most common primary malignant brain tumor in adults with high mortality. It constitutes approximately 57% of all glioma cases and 47.7% of all primary malignant central nervous system (CNS) tumors (Ostrom, Gittleman, Truitt, Boscia, Kruchko & Barnholtz-Sloan, 2018; Schaff & Mellinghoff, 2023; Tan, Ashley, Lopez, Malinzak, Friedman & Khasraw, 2020). Despite intensive treatments, including maximal safe surgical resection, followed by high-dose of radiotherapy and concomitant chemotherapy with temozolomide (TMZ), the poor prognosis of patients with GBM is dismal, with a median survival time less than 15 months and a 5-year survival rate of only 5.6% (Tan, Ashley, Lopez, Malinzak, Friedman & Khasraw, 2020). Several critical factors that limit the efficacy of treatments are: 1) GBM has an extraordinary capability of infiltrating the adjacent healthy brain areas, which precludes complete tumor resection and ultimately leads to tumor recurrence (Andrade, Chen & Jabado, 2023; Preusser et al., 2011); 2) GBM cells exhibit remarkable plasticity, which renders them to effectively adapt to the microenvironmental changes induced by conventional radiation and chemotherapy (Safa, 2015); 3) Most anti-tumor drugs including many immunotherapeutic agents cannot sufficiently cross the blood-brain barrier (BBB) and reach the tumor sites (Alexander & Cloughesy, 2017). Therefore, developing novel pharmacotherapies with adequate efficacy for patients suffering from GBM is in an urgent demand (Chokshi et al., 2021).

The inflammatory tumor microenvironment (TME), which is largely orchestrated by tumor and tumor-infiltrating immune cells, is now widely considered as an essential driving force in GBM pathogenesis, fostering tumor cell proliferation, migration, invasion, and survival (Coussens & Werb, 2002; Cui et al., 2018; Sowers, Johnson, Conrad, Patterson & Sowers, 2014). As a key inflammatory executor, cyclooxygenase (COX) is highly upregulated in intracranial tumors, particularly in GBM, and thus, was considered as a promising anti-cancer target (Palumbo et al., 2020; Qiu, Shi & Jiang, 2017). However, the therapeutic strategy of targeting COX for glioma or other inflammatory conditions has been greatly discouraged by the well-documented adverse effects of various COX inhibitors on

gastrointestinal and vascular systems (Harirforoosh, Asghar & Jamali, 2013). The untoward consequences of COX inhibition prompt us to speculate that targeting the downstream prostanoid receptors might provide alternative treatment options for GBM with higher therapeutic specificity than the general blockade of the entire COX cascade (Li et al., 2022; Qiu, Shi & Jiang, 2017).

As a major enzymatic product of COX in the brain, prostaglandin E2 (PGE_2) potentiates inflammatory responses in the occurrence of multiple malignancies and many other chronic diseases via activating four G protein-coupled receptors (GPCRs), namely EP1, EP2, EP3 and EP4 (Cook et al., 2016; Jiang, Qiu, Li & Shi, 2017; Qiu, Shi & Jiang, 2017). Notably, PGE_2 was demonstrated to promote tumorigenesis largely via acting on EP2 and EP4 in multiple malignant tumors (Ferreira et al., 2021; Hou, Yu & Jiang, 2022; Hou et al., 2022; Thumkeo et al., 2022). We previously reported that PGE_2/EP2 signaling might contribute to the malignant potential of human glioma cells, as pharmacological inhibition of EP2 receptor remarkably decreased GBM growth in both subcutaneous and intracranial tumor models (Qiu et al., 2019). In addition, recent evidence also suggests that EP4 signaling may also be involved in the onset and progression of GBM (Cook et al., 2016; Ochs et al., 2016). For instance, PGE_2-mediated induction of Id1 via EP4 is required for GBM self-renewal and radiation resistance (Cook et al., 2016). Further, EP4 is a leading $G\alpha_s$ receptor that is closely associated with the expression of tryptophan-2,3-dioxygenase (TDO) (Ochs et al., 2016), a key mediator in creating immunosuppressive environments for tumor growth, particularly in glioma (Pilotte et al., 2012; Platten, Wick & Van den Eynde, 2012; Schramme et al., 2020). Therefore, it is possible that EP4 may represent another potential target for GBM treatment. However, to best of our knowledge, the feasibility of EP4 inhibition as a therapeutic strategy has not been pharmacologically validated in animal models of GBM. In this study, we attempted to identify the characteristics of EP2 and EP4 that mediates the PGE_2 downstream cAMP signaling in human GBM cells. We also determined the therapeutic potential of the selective antagonists of EP2 and EP4 and explored the underlying mechanisms in multiple preclinical models that are relevant to human GBM.

Materials and Methods

Cell culture and chemicals

Human glioblastoma cell lines: LN229 (ATCC Cat # CRL-2611, RRID: CVCL_0393), SF767 (RRID:CVCL_6950), U87(RRID:CVCL_0022) and U251(RRID:CVCL_0021) were cultured in DMEM (Gibco, Waltham, MA, USA) supplemented with 10% (v:v) FBS (Gibco) and penicillin (100 $U \cdot mL^{-1}$)/streptomycin (100 $\mu g \cdot mL^{-1}$, Gibco) in a humidified incubator at 37 °C with 5% CO_2. PGE_2 (CAS # 363-24-6) and butaprost (CAS # 69648–38-0) were purchased from Cayman Chemical (Ann Arbor, MI, USA). Rolipram (CAS # 61413-54-5), forskolin (CAS # 66575-29-9) and luciferin (CAS # 103404-75-7) were from Sigma-Aldrich (St. Louis, MO, USA). TG6-10-1 (CAS # 1415716-58-3) and GW627368X (CAS # 439288–66-1) were obtained from MedChemExpress (Monmouth Junction, NJ, USA).

Clinical GBM tumor specimens

The human GBM tumor tissues (n = 44) and brain tissues after traumatic brain surgery (n = 11) were obtained from the tissue bank of the Affiliated Cancer Hospital of Zhengzhou University (Zhengzhou, China). The patient information, including names, ages, sex, and other personal data, was not accessible to the investigators. Based on the coded information, the patients had high-grade glioma but no history of other tumors or autoimmune diseases. In addition, the patients did not receive radiotherapy, chemotherapy, or immunotherapy before surgery. The total mRNA of GBM and control brain tissues were extracted with RNeasy Micro Kit (Qiagen, Dusseldorf, Germany), and the RNA Sequencing (RNA-seq) was performed on Illumina HiSeq 2500 after library construction.

Database

The expression levels of EP2 (encoded by *PTGER2*) and EP4 (*PTGER4*) in human GBM were analyzed using the TCGA dataset from the UCSC Xena Browser (n = 1157 for GBM samples, n = 166 for normal samples, https://xenabrowser.net/datapages/). For correlation analysis of EP2/EP4 and PD-L1 (*CD274*) in GBM, RNA-seq dataset from the UCSC Xena Browser was downloaded and analyzed using spearman's rank correlation coefficient (n = 169). The relationships between EP2 and EP4 and immune cells in human GBM samples were analyzed via ssGSEA using the TCGA RNA-seq dataset (https://portal.gdc.cancer.gov/). The correlations between EP2/EP4 and the immune infiltration levels in GBM were analyzed using TIMER database (Tumor IMmune Estimation Resource, https://cistrome.shinyapps.io/timer/).

Cell-based cAMP assay

A cell-based homogeneous time-resolved fluorescence energy transfer (TR-FRET) method was used to measure cytosol cAMP as we previously described (Jiang et al., 2010; Jiang, Van, Ganesh & Dingledine, 2018; Kang et al., 2017). In brief, human GBM cell lines LN229, SF767, U87 and U251 cells were seeded into 384-well plates (4,000 cells per well into 40 μL culture medium) and incubated overnight. Then, the medium was completely discarded and 10 μL Hanks Balanced Salt Solution (HBSS, Corning, Cat # 21–023-CV, without phenol red, Glucose 1 $g{\cdot}L^{-1}$, KCl 0.4 $g{\cdot}L^{-1}$, NaCl 8 $g{\cdot}L^{-1}$) supplemented with 20 μM rolipram were added into the wells to block PDEs that metabolize cAMP. After incubation at room temperature for 30 min, cells were treated with vehicle or tested compound for 5–10 min, followed by incubation with PGE_2 or selective EP agonists for 40 min. Samples were lysed with 10 μL lysis buffer with FRET acceptor cAMP-d2, and 1 minute later, another 10 μL lysis buffer with anti-cAMP-cryptate (Cisbio Bioassays, Cat # 62AM4PEC) was added. After incubation for 1 hour at room temperature, the FRET signal was detected by a 2104 Envision Multilabel Plate Reader (PerkinElmer) with an excitation at 340/25 nm and dual emissions at 665 and 590 nm for d2 and cryptate (100-μs delay) respectively. The FRET signal was expressed as $F665/F590 \times 10^4$.

Reverse transcriptase polymerase chain reaction (RT-PCR)

The total RNA was extracted using TRIzol (Invitrogen) with the PureLink RNA Mini Kit (Invitrogen). RNA concentration was measured using a NanoDrop

One microvolume spectrophotometer (Thermo Fisher Scientific). RNA purity was determined by the ratio of A260/A280. A total of 2 μg RNA was used to synthesize the cDNA using the SuperScript III First-Strand Synthesis SuperMix (Invitrogen) following the manual. The amplified PCR products were evaluated by 2 % agarose gel electrophoresis in Tris–acetate–EDTA (TAE) buffer stained with GelRed (Biotium). The qPCR primers for human EP2 receptor: forward, 5'-TTGGGTCTTTGCCATCCTTAG-3'; reverse, 5'- AGGAAGTTTGTGTTGCATCTTG-3'. Primers for human EP4 receptor: forward, 5'- AAAGTCCTCAGTGAGGTGGTGTC-3'; reverse, 5'- CTTGGAGGCAGGAATTTGCTT-3'. Primers for human GAPDH: forward, 5'-GTCAAGGCTGAGAACGGGAA-3'; reverse, 5'-AAATGAGCCCCAGCCTTCTC-3'.

Flow cytometry

U87 and U251 cells were seeded in 6-well plates and cultured overnight. Then the cells were treated with TG6-10-1 (10 μM) or GW627368X (10 μM). After 48 hours, cells were harvested and stained with CD44 or CD133 antibodies. Antibodies including FITC anti-human CD44 (clone BJ18, 1:100, Cat # 338803, RRID: AB_1501204), PE anti-human CD133 (clone 7, 1:100, Cat # 372803, RRID:AB_2632879) and Fc blocking solution (1:100, Cat # 422302, RRID:AB_2818986) were from BioLegend. Surface staining was done in the presence of Fc block, following CD44 and CD133 staining for 20 min at room temperature. Flow cytometry was performed on Attune NxT Flow Cytometer (Thermo Fisher Scientific, RRID:SCR_019590) and analyzed using FlowJo software (FlowJo, RRID:SCR_008520).

Colony formation assay

Human GBM cells U87 and U251 were seeded into 6-well plate and treated with TG6-10-1 (10 μM) and GW627368X (10 μM) for 7 days. The cells were stained with crystal violet and the colonies were counted under a microscope in five random fields per well at a magnification of 200×. Each condition was assessed in triplicate and repeated once.

Cell invasion assay

U87 and U251 cells were harvested and seeded into the transwell chambers that were pre-coated with Matrigel (BD Biosciences, San Jose, CA, USA). After treatment with TG6-10-1 (10 μM) or GW627368X (10 μM) for 48 hours, the cells were stained with crystal violet and counted under a microscope. Each group was assessed in triplicate and repeated three times.

Cell migration assay

Human GBM cells were seeded into the transwell chambers and treated with TG6-10-1 (10 μM) or GW627368X (10 μM). After 48 hours, the cells passing through the chamber were stained with crystal violet and counted under a microscope. Each group was assessed in triplicate and repeated three times.

Mice

Animal studies are reported in compliance with the ARRIVE2.0 and *British Journal of Pharmacology* guidelines (Percie du Sert et al., 2020) and with the recommendations made

by the *British Journal of Pharmacology* (Lilley et al., 2020). Athymic nude mice (4 weeks, female) were housed in ventilated shoebox cages (13–1/4" long × 7–1/8" wide × 5–7/16" deep; ≤ 4 mice per cage) in a pathogen-free environment at 22–24°C under a 12-hour light/dark cycle with food and water *ad libitum*. Soft bedding and environmental enrichment in the cages were provided to help to reduce stress and anxiety in the animals and to improve their welfare. Every effort was made to minimize animal suffering. For all survival surgeries including the s.c. tumor model, intracranial tumor model, and bioluminescence imaging, mice were under general anesthesia induced by isoflurane (2–5%) through an EZ-150C vaporizer (E-Z Systems). All animal procedures conformed to the institutional and IACUC guidelines of our institutions.

Subcutaneous tumor model

To generate subcutaneous (s.c.) tumors, human GBM U87 and U251 cells were inoculated into flanks (6×10^6 cells/site) while mice were anesthetized with isoflurane to enable an accurate injection. After solid tumors appeared and grew to 0.5 cm diameter, mice were randomized into three groups and treated by oral gavage for 15–20 days, with vehicle (10% PEG 200, 0.5% methylcellulose) or TG6-10-1 (10 $mg \cdot kg^{-1}$, twice a day) or GW627368X (3 $mg \cdot kg^{-1}$, once a day). Tumor growth was monitored daily by measuring tumor volume using the formula: $V = (\pi/6) \times [(A + B)/2]^3$ (A = longest diameter; B = shortest diameter). At the end of the experiments, mice were sacrificed under isoflurane anesthesia. The tumor tissues were immediately excised for further experiments.

Immunohistochemistry

The immunohistochemistry procedures were conducted in accordance with the recommendations by the *British Journal of Pharmacology (*Alexander et al., 2018). In brief, subcutaneous tumors were harvested, fixed, paraffin embedded, and sectioned (8 μm). The tumor sections were permeabilized with 0.25% Triton X-100 at room temperature for 15 min, then blocked with 10% goat serum in PBS, followed by incubation in primary antibodies at 4 °C overnight: Ki67 (1:200, Abcam, Cat # ab15580, RRID:AB_443209), CD31 (1:200, Abcam, Cat # ab28364, RRID:AB_726362), and PD-L1 (1:100, PTM BIO, Cat # PTM-5075). The sections were washed with PBS and incubated with fluorescent secondary antibody at room temperature for 2 hours, and then the immunoreactivity was detected by incubating in DAB. The stained slides were then counterstained with hematoxylin and coverslipped.

Orthotopic brain tumor model

Animals were anesthetized with isoflurane through a vaporizer and placed in a stereotaxic frame. Human GBM cells U87 and U251 labelled with luciferase (5×10^5 in 3 μL PBS) were injected into striatum of the right hemisphere (coordinates from bregma: AP = 1.0 mm; ML = +2.0 mm [right], DV = −3.0 mm) as previously described (Qiu et al., 2019). Animals were administered with buprenorphine (0.05 $mg \cdot kg^{-1}$, s.c.) twice daily for pain control for three consecutive days after surgery. After recovery from the surgery, animals were randomized and continuously treated with vehicle (10% PEG 200, 0.5% methylcellulose) or TG6-10-1 (10 $mg \cdot kg^{-1}$, twice a day) or GW627368X (3 $mg \cdot kg^{-1}$, once a day) by oral gavage for 3–4 weeks. To monitor the intracranial tumor growth, bioluminescence imaging

was conducted once a week for 3–4 weeks by a blinded investigator using an IVIS imaging system (Xenogen). Animals were anesthetized with isoflurane and injected with luciferin substrate (150 $mg \cdot kg^{-1}$, i.p.), and the bioluminescence imaging was performed 10 min later. The criteria for humane endpoint used in this study included: over 20% body weight loss, impaired locomotion, and neurological symptoms such as ataxia, lethargy, paresis, and paralysis. Mice were euthanized, by isoflurane inhalation immediately followed by decapitation, when any of these symptoms was observed, and these animals were included in the survival study.

Experimental blinding and randomization

Experimental blinding was carried out to reduce the risk of bias in this study whenever possible; the drugs used for treating animals were prepared by people who did not perform the treatments. In addition, all animals were randomized before they were treated. Results from at least seven different animals were obtained for all experimental protocols and data analyses in this study.

Statistical analysis

The sample size was calculated by power analysis with a desired power of 0.80, sigma of 0.20, and alpha of 0.05 (Faul, Erdfelder, Buchner & Lang, 2009; Faul, Erdfelder, Lang & Buchner, 2007). The data and statistical analyses comply with the recommendations of the *British Journal of Pharmacology* on experimental design and analysis in pharmacology (Curtis et al., 2022). Data retrieved from TCGA database were analyzed using R software. The correlation analyses were performed using Spearman's correlation coefficient. The concentration-response curves of tested agonists and antagonists were generated and EC_{50} values were calculated using Origin software (OriginLab, RRID:SCR_014212). Survival analyses were performed using Kaplan–Meier estimator with post hoc log-rank (Mantel-Cox) test. Statistical analyses were performed using Prism (GraphPad Software, RRID:SCR_002798). The differences were determined by one-way ANOVA with *post-hoc* Dunnett's test, Mann-Whitney U test or unpaired t test as indicated, $p < 0.05$ was considered statistically significant. Post-hoc tests were run only if F achieved $p < 0.05$ and there was no significant variance inhomogeneity. All data are presented as mean ± SEM or mean + SEM. No statistical analysis was undertaken if a dataset had a group size (n) < 5.

Nomenclature of targets and ligands

Key protein targets and ligands in this article are hyperlinked to corresponding entries in http://www.guidetopharmacology.org, and are permanently archived in the Concise Guide to PHARMACOLOGY 2021/22 (Alexander et al., 2021a; Alexander et al., 2021b).

Results

EP2 and EP4 receptors are highly upregulated in human GBM

To investigate the role of EP2 and EP4 receptors in GBM, we first examined the gene expression data in human GBM and normal brain tissues by performing RNA sequencing analysis. We observed remarkably increased expression of *PTGER2* (encoding EP2) and *PTGER4* (encoding EP4) in primary human GBM tissues compared with normal brain

tissues (Figure 1a). In line with gene profiling, the IHC staining further revealed elevated levels of EP2 and EP4 in GBM (Figure 1b). Notably, activation of EP2 and EP4 receptors in tumor cells has been reported to upregulate a variety of inflammatory cytokines, chemokines, immune checkpoints, and their corresponding receptors, thereby enhancing tumor-associated inflammation, nurturing tumor microenvironment, and facilitating tumor growth (Ma, Aoki, Tsuruyama & Narumiya, 2015). Next, we aimed to detect the expression of a range of tumor-promoting mediators that may support tumor growth, migration, invasion, angiogenesis, and immune evasion. Interestingly, spearman correlation analyses indicated the presence of significant positive correlations of expression between EP2 and EP4 receptors and all these pro-tumor factors (Figure 1c, d). Likewise, EP2 and EP4 positively correlate with the programmed death-ligand 1 (PD-L1, encoded by *CD274*) in GBM (Figure 1e, f). Given that PD-L1 is a critical immune checkpoint molecule that mediates immune escape and features as a biomarker in multiple malignant tumors (Patel & Kurzrock, 2015) and is highly regulated by PGE_2 in tumor-infiltrating myeloid cells (Prima, Kaliberova, Kaliberov, Curiel & Kusmartsev, 2017), this significant correlation might indicate the potential prognostic value of the elevated expression of EP2 and EP4 in GBM. To further validate our RNA-seq results, we assessed the expression levels of EP2 and EP4 in GBM using the TCGA dataset downloaded from the UCSC Xena Browser. Consistently, EP2 and EP4 were significantly upregulated in human GBM tumor tissues (Figure 2a).

As a major component of the TME, immune cells have been demonstrated to contribute to tumor development, immunotherapy responses, and prognosis (Zhang & Zhang, 2020). Therefore, we analyzed the correlation between EP2 and EP4 expression and tumor-infiltrating immune cells (TIICs) using the TIMER2.0 database, which is a web portal for comprehensive analysis of infiltration of immune cells, including B cells, $CD8^+$ T cells, $CD4^+$ T cells, macrophages, neutrophils, and dendritic cells (Li et al., 2020). Particularly, tumor purity is defined as the proportion of cancer cells in tumor sample, and low tumor purity is largely ascribed to increased infiltration of immune cells and indicates high malignancy (Aran, Sirota & Butte, 2015; Finocchiaro & Pellegatta, 2016). We found that the expression of EP2 and EP4 was negatively correlated with the purity of GBM, leading us to postulate that elevated levels of EP2 and EP4 may provoke more recruitment of TIICs to the tumor site. Surprisingly, the subsequent analysis revealed only one significant correlation between the EP2 expression level and the infiltration level of dendritic cells in GBM (r = 0.195, p = 5.83e-05). On the contrary, EP4 expression was significantly associated with the majority of these immune cells, with the highest significant correlation with dendritic cells (r = 0.407, p = 3.83e-18) (Figure 2b). To avoid any potential selection bias or different calculation algorithm that might be introduced by the database, we reanalyzed the correlation between EP2 and EP4 expression and infiltrating immune cells using the “single sample Gene Set Enrichment Analysis” (ssGSEA) R package. Remarkably, all immune infiltrating cells in GBM, except plasmacytoid dendritic cells (pDC), T helper 2 (Th2) cells, and NK CD56bright cells, positively correlated with EP2 and EP4 (Figure 2c). In line, PD-L1 was positively associated with EP2 and EP4 (Figure 2d). Collectively, these consistent findings suggest that elevated levels of EP2 and EP4 in GBM could upregulate

tumor-promoting mediators, facilitate more infiltration of immune cells into tumor tissues, and lead to low tumor purity along with increased malignancy in patients with GBM.

EP2 and EP4 receptors reciprocally mediate PGE_2-mediated cAMP signaling in human GBM cells

To characterize the EP2 and EP4 receptors in human GBM, we first performed RT- PCR to detect the gene expression levels of EP2 and EP4 in human GBM cell lines LN229, SF767, U87, and U251. It appeared that LN229 and U87 GBM cells expressed more EP2 than EP4 (Figure 3a). In contrast, EP4 was predominantly expressed in SF767 and U251 cells (Figure 3a). Due to the lack of EP2 antibodies suitable for western blot analysis (Varvel et al., 2021), we next focused on functional studies of EP2 and EP4 through detecting the downstream cAMP signaling. We treated these cells with a relatively high concentration (10 μM) of PGE_2, selective EP2 receptor agonist butaprost, or EP4 agonist CAY10598, aiming to fully activate their EP2 and EP4 receptors. The cAMP levels were detected via a time-resolved fluorescence energy transfer (TR-FRET) assay, in which a decline of the FRET signal represents an increase of cAMP level. Forskolin is a direct activator of adenylyl cyclases and is commonly used to indicate the maximal capability of the cells to produce cAMP. We found that PGE_2-induced cAMP accumulation in all examined human GBM cell lines to a similar degree of forskolin (Figure 3b). Intriguingly, the dominant subtype EP receptor that mediates PGE_2-initiated cAMP signaling showed a discrepancy pattern in these GBM cells. Specifically, EP2 agonist butaprost, and to a lesser extent, EP4 agonist CAY10598, induced cAMP accumulation in LN229 and U87 cells (Figure 3c). In contrast, stimulation with EP4 agonist CAY10598 led to substantial more cAMP production than EP2 agonist butaprost in SF767 and U251 cells (Figure 3c). Thus, EP2 in LN229 and U87 cells, whereas EP4 in SF767 and U251 cells, is the dominant $G\alpha_s$-coupled receptor that transduces the PGE_2 signal. To further explore the functional role of EP2 and EP4 receptors, we next focused on the GBM cell lines U87 and U251. The TR-FRET assay on U87 cells revealed that PGE_2 and butaprost induced cAMP production clearly in a concentration-dependent manner, whereas the dose-responsive curve was blunted in CAY10598 treatment group (Figure 3d). Conversely, in the U251 cells, PGE_2 and CAY10598, but not butaprost, promoted cAMP production in a concentration-dependent manner (Figure 3d).

We previously reported that TG6-10-1, a small-molecule antagonist of EP2 receptor, was able to largely prevent the PGE_2-induced cAMP in LN229 cells but its effect in SF767 cells was much less, suggesting that another PGE_2 receptor (likely EP4) might be involved in cAMP signaling in these cells (Qiu et al., 2019). To investigate this possibility, we tested TG6-10-1 along with a selective EP4 antagonist GW627368X for their effects on cAMP in GBM cells that were stimulated with 1 μM PGE_2 aiming to induce the maximal cytosol cAMP. Interestingly, TG6-10-1 and GW627368X at 1 μM exhibited robust inhibition on PGE_2-induced cAMP production in human GBM cell lines U87 and U251, respectively (Figure 3e). Notably, the inhibition of EP2 receptor by TG6-10-1, other than EP4 inhibition by GW627368X, was able to robustly decrease PGE_2-induced cAMP signaling in U87 cells in a concentration-dependent manner (Figure 3f). On the contrary, in U251 cells, both TG6-10-1 and GW627368X suppressed PGE_2-mediated cAMP production but with higher potency and efficacy observed in GW627368X-treated cells (Figure 3f). These

results together suggest that PGE_2 receptors EP2 and EP4 may complementarily mediate cAMP signaling in human GBMs and can be efficiently blocked by selective EP2 and EP4 antagonists.

Inhibition of EP2 and EP4 receptors suppresses PGE_2 activity-mediated tumorigenicity in human GBM

To investigate the effects of EP2 and EP4 inhibition on GBM cell colony formation, U87 and U251 cells were seeded into 6-well plate and treated with TG6-10-1 or GW627368X for 7 days. Compared with control groups, TG6-10-1 and GW627368X substantially attenuated the colony formation in U87 and U251 cells, respectively (Figure 4a). These findings suggest PGE_2 signaling via EP2 and EP4 receptors may involve in the tumor initiation and self-renewal of GBM cells, which are the hallmarks of cancer stem cell (CSC). For this end, we detected the expression of CSC markers CD44 and CD133 in U87 and U251 cells treated with EP2 and EP4 antagonists. The results showed that EP2 antagonist TG6-10-1, but not EP4 antagonist GW627368X, profoundly inhibited the expression levels of CD44 and CD133 in U87 cells (Figure 4b, c). Conversely, EP4 inhibition by GW627368X largely suppresses the expression levels of CD44 and CD133 in U251 cells (Figure 4b, c). We also studied the effect of EP2 and EP4 inhibition on GBM cell invasion and found that TG6-10-1 significantly inhibited the cell invasion of U87 cells but had no effect on U251 cells. In contrast, GW627368X suppressed the cell invasion of U251 without affecting U87 cells (Figure 5a). Finally, we examined whether blocking EP2 and EP4 signaling could dampen the GBM cell migration. In line, EP2 antagonist TG6-10-1 greatly inhibited the cell migration of U87, while this effect was observed in U251 cells when treated with EP4 antagonist GW627368X (Figure 5b). The results from these *in vitro* assays together suggest that the PGE_2 activity-mediated tumorigenicity in human glioblastoma cells, including tumor initiation, invasion, and migration, can largely be attributed to the activation of EP2 and EP4 receptors.

Inhibiting EP2 and EP4 receptors blocks GBM cell growth *in vivo*

To determine the role of EP2 and EP4 receptors in GBM growth *in vivo*, the subcutaneous tumor models of U87 and U251 cells were established in athymic nude mice. The mice were then randomly divided into three groups, followed by treatment with vehicle (10% PEG 200, 0.5% methylcellulose), TG6-10-1 (10 $mg{\cdot}kg^{-1}$, twice a day), or GW627368X (3 $mg{\cdot}kg^{-1}$, once a day). After approximately 3 weeks of treatment, all tumors were harvested, weighed, and analyzed. Other than the tumor burden, mice were overall healthy and did not exhibit any behavioral abnormalities or significant weight loss. We first found that TG6-10-1 considerably inhibited the tumor growth formed by U87 cells ($p < 0.05$ at days 15–19; Figure 6a, b), whereas GW627368X largely reduced the tumor growth of U251 ($p < 0.05$ at days 6–15; Figure 6e, f), when compared to their corresponding vehicle-treated control groups. In line, treatment with TG6-10-1 and GW627368X on average decreased the weight of U87 tumors by 45% ($p = 0.0305$; Figure 6c), and U251 tumors by 65% ($p < 0.0001$; Figure 6g), respectively.

Intriguingly, GW627368X had no effect on tumors formed by U87 GBM cells (Figure 6a–c), in which the expression of functional EP4 was relatively low (Figure 3a–c). Likewise,

treatment with TG6-10-1 only showed minimal suppression on xenografts produced by U251 cells (Figure 6e–g), which expressed more functional EP4 receptors than EP2 (Figure 3a–c). Thus, whether the treatment with these two antagonists can lead to any therapeutic effects mainly depends on the expression of their intended targets in the GBM cells used for the models. Nonetheless, these findings together suggest that PGE_2-cAMP signaling via EP2 and EP4 is involved in GBM growth, and EP2 and EP4 receptors might represent potential therapeutic targets for GBM treatment.

We next performed immunohistochemistry (IHC) to examine the effects of EP2 and EP4 inhibition on the proliferative index of GBM cells in vivo. Immunostaining of Ki-67, a nuclear protein widely used as proliferation indicator, was used to identify the proliferating cells in subcutaneous GBM tissues. We found that systemic treatment with TG6-10-1, but not GW627368X, substantially decreased the number of Ki67 positive cells in U87 cells-derived xenografts (Figure 6d), whereas the opposite effects by these two compounds were observed in U251 cells-derived tumors (Figure 6h).

We then evaluated the effects of EP2 and EP4 inhibition on the expression of PD-L1 in subcutaneous tumors. The immunostaining results revealed that levels of PD-L1 were decreased in U87 and U251 tumors blocked by TG6-10-1 and GW627368X, respectively (Figure 6d, h). Considering a key role of PGE_2 in the regulation of PD-L1 expression in tumor-associated macrophages and myeloid-derived suppressor cells (Prima, Kaliberova, Kaliberov, Curiel & Kusmartsev, 2017), these interesting findings indicate the possible presence of immune suppression induced by PD-L1 to promote tumor immune evasion and enhance tumor growth, which might be mediated by EP2 and EP4 receptors in PGE_2 signaling-associated tumorigenesis of GBM.

Angiogenesis represents a hallmark of malignant tumors and is a critical feature of glioblastomas (Ahir, Engelhard & Lakka, 2020). The expression of the PECAM1 or CD31, has been widely used as a common biomarker for microvascular proliferation in various tumors (Zhang et al., 2018). Therefore, we were interested in determining whether PGE_2 signaling via EP2 and EP4 receptors contributes to the elevation of CD31 in GBM. We performed IHC staining of CD31 in xenograft tissues. We found that TG6-10-1 and GW627368X largely reduced the CD31 positive cells in xenograft samples formed by U87 and U251 cells (Figure 6d, h), respectively. To further verify the roles of EP2 and EP4 in vascular formation, we analyzed the correlation of expression between angiogenesis-related genes with EP2 and EP4 in human GBM using the TCGA dataset. We observed that endothelial growth factor C (*VEGFC*), angiopoietin 1 (*ANGPT1*), platelet-derived growth factor receptor beta (*PDGFRB*), endoglin (*ENG*), insulin-like growth factors 1 and 2 (*IGF1*, *IGF2*) and CD31(*PECAM1*) were positively associated with EP2 and EP4 (Figure 7). Together, our results suggest an essential role for EP2 and EP4 receptors in PGE_2 activity-associated angiogenesis of glioblastoma.

Inhibiting EP2 and EP4 receptors diminishes orthotopic GBM

We next assessed the effects of TG6-10-1 and GW627368X in an orthotopic GBM model because the orthotopic xenografts are considered to better mimic the original tumor conditions, particularly the tumor microenvironments, than the subcutaneous tumors. Firstly,

U87 and U251 cells were labeled with luciferase and were intracranially injected into the nude mice. Following the recovery from surgery, the animals were randomly divided into three groups and treated with vehicle (10% PEG 200, 0.5% methylcellulose), TG6-10-1 (10 $mg \cdot kg^{-1}$, twice a day) or GW627368 (3 $mg \cdot kg^{-1}$, once a day) through oral gavage for 3–4 weeks. Utilizing a Xenogen IVIS system, the bioluminescence signal of the intracranial tumors was monitored weekly. The results showed that the orthotopic tumors formed by U87 (Figure 8a) and U251 (Figure 8d) cells progressed aggressively, demonstrated by continually increased intracranial bioluminescence signal over the 3-week detection period. However, TG6-10-1 treatment substantially suppressed the growth of the U87 tumors compared to the vehicle group (Figure 8b). In contrast, GW627368X treatment significantly inhibited the growth of intracranial U251 tumors (Figure 8e). Furthermore, survival analysis using Kaplan–Meier estimator showed that treatment with TG6-10-1 for only 3 weeks prolonged survival of U87-harboring mice ($p < 0.001$; Figure 8c), the median survival times of tumor-harboring mice treated by vehicle ($n = 7$), GW627368X ($n = 7$) and TG6-10-1 ($n = 7$) were 21, 22 and 27 days, respectively. Similarly, U251-harboring mice exhibited increased survival when treated with GW627368X for 4 weeks ($p < 0.001$; Figure 8f), and the median survival times of tumor-harboring mice treated by vehicle ($n = 7$), GW627368X ($n = 7$) and TG6-10-1 ($n = 7$) were 28, 60 and 31 days, respectively. It appears that U87 cells displayed more aggressive ability than U251 glioma cells when grown in orthotopic conditions, as revealed by overall lower median survival rates in mice with U87 cells (Figure 8c, f). Taken together, the results of subcutaneous and orthotopic xenograft models suggest that inhibiting PGE_2 signaling using selective EP2 and EP4 antagonists suppresses tumor growth of GBM *in vivo*.

Discussion

In the present study, we performed comprehensive data analyses of gene expression utilizing bioinformatics approaches based on our RNA sequencing results and publicly available TCGA database, and the results led us to hypothesize that PGE_2 signaling via EP2 and EP4 receptors play essential roles in tumor growth of GBM. We first tested this hypothesis and demonstrated that EP2 and EP4 complementarily regulate PGE_2/cAMP signaling in various human GBM cells. In addition, inhibition of EP2 and EP4 receptors by small-molecular antagonists TG6-10-1 and GW627368X significantly suppressed the tumorigenicity of GBM cells *in vitro* and *in vivo*. Our results also showed that blocking PGE_2 signaling via inhibiting EP2 and EP4 exhibited anti-proliferative, anti-invasion, anti-migration, and anti-angiogenic effects in our multiple GBM models, which may elucidate the mechanisms of their anti-GBM actions. These findings suggest that targeting both EP2 and EP4 receptors may provide potential novel therapeutical options for patients with GBM.

The COX activity is often upregulated and highly correlates with the cell proliferation, invasion, migration, angiogenesis, immune evasion, and poor prognosis of human GBM (Majchrzak-Celinska et al., 2021; Yin et al., 2021). COX thus was once regarded as an appealing therapeutic target for CNS tumors. However, the untoward consequences of blocking COX activity by nonsteroidal anti-inflammatory drugs (NSAIDs) or selective COX-2 inhibitors (Coxibs) have dampened their clinical applications in tumor treatment (Qiu, Shi & Jiang, 2017). The severe side effects of long-term consumption of these drugs

include but are not limited to myocardial infarction, stroke, gastrointestinal bleeding, and even mortality (Bindu, Mazumder & Bandyopadhyay, 2020; Grosser, Yu & Fitzgerald, 2010). The disturbing consequences of long-term inhibition of COX-2 on the microvascular systems have led to the subsequent withdrawal of two legendary COX-2 inhibitors, rofecoxib and valdecoxib in the past two decades; celecoxib remains available but with an FDA-mandated "black box warning" for cardiovascular risk. The downstream signaling of COX is mediated by five types of prostanoids that, in turn, can activate a panel of nine GPCRs, executing a myriad of detrimental and beneficial actions (Dey, Kang, Qiu, Du & Jiang, 2016; Jiang & Dingledine, 2013). The *Jekyll and Hyde* nature of COX cascade inspires us and many others to seek for the next-generation therapeutic targets from its downstream prostanoid synthases or receptors (Hou, Yu & Jiang, 2022; Jiang, Qiu, Li & Shi, 2017). As such, blocking PGE_2 receptors EP2 and EP4 might represent an alternative therapeutic strategy to suppress GBM tumor growth.

PGE_2 is the most abundant prostaglandin commonly found at various tumor sites (Reader, Holt & Fulton, 2011), where it has been shown to promote tumorigenesis via all four EP receptors. Among these, the $G\alpha_s$-coupled EP2 and EP4 receptors have been mostly investigated for their essential roles in the development and progression of tumors, including those of head, lung, stomach, skin, ovary, and prostate (Jiang & Dingledine, 2013; Take, Koizumi & Nagahisa, 2020; Wang, Morris, Bode & Zhang, 2022). Interestingly, our current work unraveled differential expression of the dominant $G\alpha_s$-coupled PGE_2 receptor in various human GBM cell lines: EP2 in LN229 and U87 cells; EP4 in SF767 and U251 cells. Inhibition of the dominant PGE_2 receptor (EP2 or EP4) is sufficient to suppress tumor progression in our subcutaneous and orthotopic GBM models. However, due to the limited cell lines examined in this study, we cannot exclude the possibility that EP2 and EP4 might equally contribute to pro-tumor activities in some GBM cell lines. If this is the case, blocking EP2 or EP4 alone may not be able to effectively impair tumor growth in GBM patients. To address this concern, future study should be also directed to explore the anti-tumor effects of simultaneously blocking both EP2 and EP4 receptors on GBM tumor growth by a dual antagonist, e.g., TPST-1495, which is currently under clinical trial for treatment of various solid cancers (https://clinicaltrials.gov/ct2/show/NCT04344795), or by combined treatment with separate EP2 and EP4 antagonists as recently reported (Kourpa et al., 2023; Thumkeo et al., 2022).

Recently, PGE_2 signaling-nurturing tumor microenvironments have emerged as an essential contributor to tumor growth through multiple mechanisms: (1) inducing reactive mediators for cancer cell growth, including pro-inflammatory cytokines, chemokines, and growth factors (Mantovani, Allavena, Sica & Balkwill, 2008); (2) facilitating angiogenesis via acting on VEGF receptors (Gately & Li, 2004); (3) creating immunosuppressive microenvironments allowing tumor cells to escape the immunosurveillance (Zelenay et al., 2015). However, the molecular mechanisms whereby PGE_2/EP/cAMP signaling promotes GBM progression remain unclear. Here, we demonstrated positive correlations between EP2/EP4 receptors and a myriad of essential tumor-promoting cytokines, chemokines, and corresponding receptors (Figure 1c, d). In addition, the expression of EP2 and EP4 is highly correlated with the most pronounced angiogenesis biomarker, CD31 (PECAM-1), supporting an angiogenic role of EP2 and EP4 in GBM. The potential engagement of EP2

and EP4 in microvascular proliferation of GBM was further substantiated by evidence that pharmacological inhibition of EP2 and EP4 receptors reduced the CD31 levels in GBM xenografts (Figure 6d, h).

The expression levels of PD-L1 were also decreased in U87 and U251 tumors by blocking EP2 and EP4, respectively. However, whether the PD-L1-promoted immune suppression leads to tumor escape from immune surveillance and contributes to EP2 or EP4-mediated GBM growth remains to be determined in future studies. Nevertheless, this work provides proof-of-concept evidence that PGE_2 signaling via EP2 and EP4 receptors might represent appealing anti-inflammatory targets for patients with GBM. Our findings also suggest that targeting both EP2 and EP4 receptors might provide a more effective strategy than inhibiting either EP2 or EP4 alone because the expression of EP2 and EP4 may vary in different GBM tumors.

Acknowledgements

This work was partially supported by internal funds from Zhengzhou University (J.Q.), University of Cincinnati College of Pharmacy (J.J.) and University of Tennessee College of Pharmacy (J.J.), and the National Institute of Neurological Disorders and Stroke (NINDS) grant R01NS100947 (J.J.).

Declaration of transparency and scientific rigour

This Declaration acknowledges that this paper adheres to the principles for transparent reporting and scientific rigour of preclinical research as stated in the BJP guidelines for Design and Analysis, Immunoblotting and Immunochemistry, and Animal Experimentation, and as recommended by funding agencies, publishers and other organizations engaged with supporting research.

Data availability statement

The data that support the findings of this study are available from the corresponding authors upon reasonable request.

Abbreviations

GBM	glioblastoma
COX	cyclooxygenase
PGE_2	prostaglandin E2
TMZ	temozolomide
BBB	blood-brain barrier
TME	tumor microenvironment
NSAIDs	non-steroidal anti-inflammatory drugs
GPCRs	G protein-coupled receptors
cAMP	cyclic AMP
TR-FRET	time-resolved fluorescence energy transfer

i.p.	intraperitoneal
s.c.	subcutaneous
IHC	immunohistochemistry
PD-L1	programmed death ligand 1
TIICs	tumor-infiltrating immune cells
pDC	plasmacytoid dendritic cells
Th2	T helper 2 cells
TCGA	The Cancer Genome Atlas

References

Ahir BK, Engelhard HH, & Lakka SS (2020). Tumor Development and Angiogenesis in Adult Brain Tumor: Glioblastoma. Mol Neurobiol 57: 2461–2478. 10.1007/s12035-020-01892-8 [PubMed: 32152825]

Alexander Roberts RE, Broughton BRS Sobey CG, George CH Stanford SC, et al. (2018). Goals and practicalities of immunoblotting and immunohistochemistry: A guide for submission to the British Journal of Pharmacology. Br J Pharmacol 175: 407–411. 10.1111/bph.14112 [PubMed: 29350411]

Alexander BM, & Cloughesy TF (2017). Adult Glioblastoma. J Clin Oncol 35: 2402–2409. 10.1200/JCO.2017.73.0119 [PubMed: 28640706]

Alexander SP, Christopoulos A, Davenport AP, Kelly E, Mathie A, Peters JA, et al. (2021a). THE CONCISE GUIDE TO PHARMACOLOGY 2021/22: G protein-coupled receptors. Br J Pharmacol 178 Suppl 1: S27–S156. 10.1111/bph.15538 [PubMed: 34529832]

Alexander SP, Fabbro D, Kelly E, Mathie A, Peters JA, Veale EL, et al. (2021b). THE CONCISE GUIDE TO PHARMACOLOGY 2021/22: Enzymes. Br J Pharmacol 178 Suppl 1: S313–S411. 10.1111/bph.15542 [PubMed: 34529828]

Andrade AF, Chen CCL, & Jabado N (2023). Oncohistones in brain tumors: the soil and seed. Trends Cancer 9: 444–455. 10.1016/j.trecan.2023.02.003 [PubMed: 36933956]

Aran D, Sirota M, & Butte AJ (2015). Systematic pan-cancer analysis of tumour purity. Nat Commun 6: 8971. 10.1038/ncomms9971 [PubMed: 26634437]

Bindu S, Mazumder S, & Bandyopadhyay U (2020). Non-steroidal anti-inflammatory drugs (NSAIDs) and organ damage: A current perspective. Biochem Pharmacol 180: 114147. 10.1016/j.bcp.2020.114147 [PubMed: 32653589]

Chokshi CR, Brakel BA, Tatari N, Savage N, Salim SK, Venugopal C, et al. (2021). Advances in Immunotherapy for Adult Glioblastoma. Cancers (Basel) 13: 3400. 10.3390/cancers13143400 [PubMed: 34298615]

Cook PJ, Thomas R, Kingsley PJ, Shimizu F, Montrose DC, Marnett LJ, et al. (2016). Cox-2-derived PGE2 induces Id1-dependent radiation resistance and self-renewal in experimental glioblastoma. Neuro Oncol 18: 1379–1389. 10.1093/neuonc/now049 [PubMed: 27022132]

Coussens LM, & Werb Z (2002). Inflammation and cancer. Nature 420: 860–867. 10.1038/nature01322 [PubMed: 12490959]

Cui X, Morales RT, Qian W, Wang H, Gagner JP, Dolgalev I, et al. (2018). Hacking macrophage-associated immunosuppression for regulating glioblastoma angiogenesis. Biomaterials 161: 164–178. 10.1016/j.biomaterials.2018.01.053 [PubMed: 29421553]

Curtis MJ, Alexander SPH, Cirino G, George CH, Kendall DA, Insel PA, et al. (2022). Planning experiments: Updated guidance on experimental design and analysis and their reporting III. Br J Pharmacol 179: 3907–3913. 10.1111/bph.15868 [PubMed: 35673806]

Dey A, Kang X, Qiu J, Du Y, & Jiang J (2016). Anti-Inflammatory Small Molecules To Treat Seizures and Epilepsy: From Bench to Bedside. Trends Pharmacol Sci 37: 463–484. 10.1016/j.tips.2016.03.001 [PubMed: 27062228]

Faul F, Erdfelder E, Buchner A, & Lang AG (2009). Statistical power analyses using G*Power 3.1: tests for correlation and regression analyses. Behav Res Methods 41: 1149–1160. 10.3758/BRM.41.4.1149 [PubMed: 19897823]

Faul F, Erdfelder E, Lang AG, & Buchner A (2007). G*Power 3: a flexible statistical power analysis program for the social, behavioral, and biomedical sciences. Behav Res Methods 39: 175–191. 10.3758/bf03193146 [PubMed: 17695343]

Ferreira MT, Miyake JA, Gomes RN, Feitoza F, Stevannato PB, da Cunha AS, et al. (2021). Cyclooxygenase Inhibition Alters Proliferative, Migratory, and Invasive Properties of Human Glioblastoma Cells In Vitro. Int J Mol Sci 22. 10.3390/ijms22094297

Finocchiaro G, & Pellegatta S (2016). Immunotherapy with dendritic cells loaded with glioblastoma stem cells: from preclinical to clinical studies. Cancer Immunol Immunother 65: 101–109. 10.1007/s00262-015-1754-9 [PubMed: 26377689]

Gately S, & Li WW (2004). Multiple roles of COX-2 in tumor angiogenesis: a target for antiangiogenic therapy. Semin Oncol 31: 2–11. 10.1053/j.seminoncol.2004.03.040

Grosser T, Yu Y, & Fitzgerald GA (2010). Emotion recollected in tranquility: lessons learned from the COX-2 saga. Annu Rev Med 61: 17–33. 10.1146/annurev-med-011209-153129 [PubMed: 20059330]

Harirforoosh S, Asghar W, & Jamali F (2013). Adverse effects of nonsteroidal antiinflammatory drugs: an update of gastrointestinal, cardiovascular and renal complications. J Pharm Pharm Sci 16: 821–847. 10.18433/j3vw2f [PubMed: 24393558]

Hou R, Yu Y, & Jiang J (2022). Prostaglandin E2 in neuroblastoma: Targeting synthesis or signaling? Biomed Pharmacother 156: 113966. 10.1016/j.biopha.2022.113966 [PubMed: 36411643]

Hou R, Yu Y, Sluter MN, Li L, Hao J, Fang J, et al. (2022). Targeting EP2 receptor with multifaceted mechanisms for high-risk neuroblastoma. Cell Rep 39: 111000. 10.1016/j.celrep.2022.111000 [PubMed: 35732130]

Jiang J, & Dingledine R (2013). Prostaglandin receptor EP2 in the crosshairs of anti-inflammation, anti-cancer, and neuroprotection. Trends Pharmacol Sci 34: 413–423. 10.1016/j.tips.2013.05.003 [PubMed: 23796953]

Jiang J, Ganesh T, Du Y, Thepchatri P, Rojas A, Lewis I, et al. (2010). Neuroprotection by selective allosteric potentiators of the EP2 prostaglandin receptor. Proc Natl Acad Sci U S A 107: 2307–2312. 10.1073/pnas.0909310107 [PubMed: 20080612]

Jiang J, Qiu J, Li Q, & Shi Z (2017). Prostaglandin E2 Signaling: Alternative Target for Glioblastoma? Trends Cancer 3: 75–78. 10.1016/j.trecan.2016.12.002 [PubMed: 28718447]

Jiang J, Van TM, Ganesh T, & Dingledine R (2018). Discovery of 2-Piperidinyl Phenyl Benzamides and Trisubstituted Pyrimidines as Positive Allosteric Modulators of the Prostaglandin Receptor EP2. ACS Chem Neurosci 9: 699–707. 10.1021/acschemneuro.7b00486 [PubMed: 29292987]

Kang X, Qiu J, Li Q, Bell KA, Du Y, Jung DW, et al. (2017). Cyclooxygenase-2 contributes to oxidopamine-mediated neuronal inflammation and injury via the prostaglandin E2 receptor EP2 subtype. Sci Rep 7: 9459. 10.1038/s41598-017-09528-z [PubMed: 28842681]

Kourpa A, Schulz A, Mangelsen E, Kaiser-Graf D, Koppers N, Stoll M, et al. (2023). Studies in Zebrafish and Rat Models Support Dual Blockade of EP2 and EP4 (Prostaglandin E(2) Receptors Type 2 and 4) for Renoprotection in Glomerular Hyperfiltration and Albuminuria. Hypertension 80: 771–782. 10.1161/HYPERTENSIONAHA.122.20392 [PubMed: 36715011]

Li L, Yasmen N, Hou R, Yang S, Lee JY, Hao J, et al. (2022). Inducible Prostaglandin E Synthase as a Pharmacological Target for Ischemic Stroke. Neurotherapeutics 19: 366–385. 10.1007/s13311-022-01191-1 [PubMed: 35099767]

Li T, Fu J, Zeng Z, Cohen D, Li J, Chen Q, et al. (2020). TIMER2.0 for analysis of tumor-infiltrating immune cells. Nucleic Acids Res 48: W509–W514. 10.1093/nar/gkaa407 [PubMed: 32442275]

Lilley E, Stanford SC, Kendall DE, Alexander SPH, Cirino G, Docherty JR, et al. (2020). ARRIVE 2.0 and the British Journal of Pharmacology: Updated guidance for 2020. Br J Pharmacol 177: 3611–3616. 10.1111/bph.15178 [PubMed: 32662875]

Ma X, Aoki T, Tsuruyama T, & Narumiya S (2015). Definition of Prostaglandin E2-EP2 Signals in the Colon Tumor Microenvironment That Amplify Inflammation and Tumor Growth. Cancer Res 75: 2822–2832. 10.1158/0008-5472.CAN-15-0125 [PubMed: 26018088]

Majchrzak-Celinska A, Misiorek JO, Kruhlenia N, Przybyl L, Kleszcz R, Rolle K, et al. (2021). COXIBs and 2,5-dimethylcelecoxib counteract the hyperactivated Wnt/beta-catenin pathway and COX-2/PGE2/EP4 signaling in glioblastoma cells. BMC Cancer 21: 493. 10.1186/s12885-021-08164-1 [PubMed: 33941107]

Mantovani A, Allavena P, Sica A, & Balkwill F (2008). Cancer-related inflammation. Nature 454: 436–444. 10.1038/nature07205 [PubMed: 18650914]

Ochs K, Ott M, Rauschenbach KJ, Deumelandt K, Sahm F, Opitz CA, et al. (2016). Tryptophan-2,3-dioxygenase is regulated by prostaglandin E2 in malignant glioma via a positive signaling loop involving prostaglandin E receptor-4. J Neurochem 136: 1142–1154. 10.1111/jnc.13503 [PubMed: 26708701]

Ostrom QT, Gittleman H, Truitt G, Boscia A, Kruchko C, & Barnholtz-Sloan JS (2018). CBTRUS Statistical Report: Primary Brain and Other Central Nervous System Tumors Diagnosed in the United States in 2011–2015. Neuro Oncol 20: iv1–iv86. 10.1093/neuonc/noy131 [PubMed: 30445539]

Palumbo P, Lombardi F, Augello FR, Giusti I, Dolo V, Leocata P, et al. (2020). Biological effects of selective COX-2 inhibitor NS398 on human glioblastoma cell lines. Cancer Cell Int 20: 167. 10.1186/s12935-020-01250-7 [PubMed: 32435158]

Patel SP, & Kurzrock R (2015). PD-L1 Expression as a Predictive Biomarker in Cancer Immunotherapy. Mol Cancer Ther 14: 847–856. 10.1158/1535-7163.MCT-14-0983 [PubMed: 25695955]

Percie du Sert N, Hurst V, Ahluwalia A, Alam S, Avey MT, Baker M, et al. (2020). The ARRIVE guidelines 2.0: Updated guidelines for reporting animal research. Br J Pharmacol 177: 3617–3624. 10.1111/bph.15193 [PubMed: 32662519]

Pilotte L, Larrieu P, Stroobant V, Colau D, Dolusic E, Frederick R, et al. (2012). Reversal of tumoral immune resistance by inhibition of tryptophan 2,3-dioxygenase. Proc Natl Acad Sci U S A 109: 2497–2502. 10.1073/pnas.1113873109 [PubMed: 22308364]

Platten M, Wick W, & Van den Eynde BJ (2012). Tryptophan catabolism in cancer: beyond IDO and tryptophan depletion. Cancer Res 72: 5435–5440. 10.1158/0008-5472.CAN-12-0569 [PubMed: 23090118]

Preusser M, de Ribaupierre S, Wohrer A, Erridge SC, Hegi M, Weller M, et al. (2011). Current concepts and management of glioblastoma. Ann Neurol 70: 9–21. 10.1002/ana.22425 [PubMed: 21786296]

Prima V, Kaliberova LN, Kaliberov S, Curiel DT, & Kusmartsev S (2017). COX2/mPGES1/PGE2 pathway regulates PD-L1 expression in tumor-associated macrophages and myeloid-derived suppressor cells. Proc Natl Acad Sci U S A 114: 1117–1122. 10.1073/pnas.1612920114 [PubMed: 28096371]

Qiu J, Li Q, Bell KA, Yao X, Du Y, Zhang E, et al. (2019). Small-molecule inhibition of prostaglandin E receptor 2 impairs cyclooxygenase-associated malignant glioma growth. Br J Pharmacol 176: 1680–1699. 10.1111/bph.14622 [PubMed: 30761522]

Qiu J, Shi Z, & Jiang J (2017). Cyclooxygenase-2 in glioblastoma multiforme. Drug Discov Today 22: 148–156. 10.1016/j.drudis.2016.09.017 [PubMed: 27693715]

Reader J, Holt D, & Fulton A (2011). Prostaglandin E2 EP receptors as therapeutic targets in breast cancer. Cancer Metastasis Rev 30: 449–463. 10.1007/s10555-011-9303-2 [PubMed: 22002714]

Safa AR (2015). Glioblastoma stem cells (GSCs) epigenetic plasticity and interconversion between differentiated non-GSCs and GSCs. Genes Dis 2: 152–163. 10.1016/j.gendis.2015.02.001 [PubMed: 26137500]

Schaff LR, & Mellinghoff IK (2023). Glioblastoma and Other Primary Brain Malignancies in Adults: A Review. JAMA 329: 574–587. 10.1001/jama.2023.0023 [PubMed: 36809318]

Schramme F, Crosignani S, Frederix K, Hoffmann D, Pilotte L, Stroobant V, et al. (2020). Inhibition of Tryptophan-Dioxygenase Activity Increases the Antitumor Efficacy of Immune Checkpoint Inhibitors. Cancer Immunol Res 8: 32–45. 10.1158/2326-6066.CIR-19-0041 [PubMed: 31806638]

Sowers JL, Johnson KM, Conrad C, Patterson JT, & Sowers LC (2014). The role of inflammation in brain cancer. Adv Exp Med Biol 816: 75–105. 10.1007/978-3-0348-0837-8_4 [PubMed: 24818720]

Take Y, Koizumi S, & Nagahisa A (2020). Prostaglandin E Receptor 4 Antagonist in Cancer Immunotherapy: Mechanisms of Action. Front Immunol 11: 324. 10.3389/fimmu.2020.00324 [PubMed: 32210957]

Tan AC, Ashley DM, Lopez GY, Malinzak M, Friedman HS, & Khasraw M (2020). Management of glioblastoma: State of the art and future directions. CA Cancer J Clin 70: 299–312. 10.3322/caac.21613 [PubMed: 32478924]

Thumkeo D, Punyawatthananukool S, Prasongtanakij S, Matsuura R, Arima K, Nie H, et al. (2022). PGE(2)-EP2/EP4 signaling elicits immunosuppression by driving the mregDC-Treg axis in inflammatory tumor microenvironment. Cell Rep 39: 110914. 10.1016/j.celrep.2022.110914 [PubMed: 35675777]

Varvel NH, Espinosa-Garcia C, Hunter-Chang S, Chen D, Biegel A, Hsieh A, et al. (2021). Peripheral Myeloid Cell EP2 Activation Contributes to the Deleterious Consequences of Status Epilepticus. J Neurosci 41: 1105–1117. 10.1523/JNEUROSCI.2040-20.2020 [PubMed: 33293358]

Wang Q, Morris RJ, Bode AM, & Zhang T (2022). Prostaglandin Pathways: Opportunities for Cancer Prevention and Therapy. Cancer Res 82: 949–965. 10.1158/0008-5472.CAN-21-2297 [PubMed: 34949672]

Yin D, Jin G, He H, Zhou W, Fan Z, Gong C, et al. (2021). Celecoxib reverses the glioblastoma chemo-resistance to temozolomide through mitochondrial metabolism. Aging (Albany NY) 13: 21268–21282. 10.18632/aging.203443 [PubMed: 34497154]

Zelenay S, van der Veen AG, Bottcher JP, Snelgrove KJ, Rogers N, Acton SE, et al. (2015). Cyclooxygenase-Dependent Tumor Growth through Evasion of Immunity. Cell 162: 1257–1270. 10.1016/j.cell.2015.08.015 [PubMed: 26343581]

Zhang Y, & Zhang Z (2020). The history and advances in cancer immunotherapy: understanding the characteristics of tumor-infiltrating immune cells and their therapeutic implications. Cell Mol Immunol 17: 807–821. 10.1038/s41423-020-0488-6 [PubMed: 32612154]

Zhang YY, Kong LQ, Zhu XD, Cai H, Wang CH, Shi WK, et al. (2018). CD31 regulates metastasis by inducing epithelial-mesenchymal transition in hepatocellular carcinoma via the ITGB1-FAK-Akt signaling pathway. Cancer Lett 429: 29–40. 10.1016/j.canlet.2018.05.004 [PubMed: 29746931]

What is already known?

- PGE_2-mediated $G\alpha_s$-dependent signaling via EP2 and EP4 receptors plays an essential role in the development and progression of multiple tumor types.
- EP2 receptor activation has emerged as a critical driving force for gliomagenesis.
- Pharmacological inhibition of EP2 receptor significantly suppresses GBM growth.

What does this study add?

- Both EP2 and EP4 receptors are highly upregulated and positively correlate with a variety of tumor-promoting molecules and tumor-infiltrating immune cells in human GBM.
- EP2 and EP4 receptors complementarily mediate PGE_2-elicited cAMP signaling in human glioblastoma cells.
- Inhibiting EP2 and EP4 receptors impairs glioblastoma growth in multiple GBM models.

What is the clinical significance?

- Targeting either EP2 or EP4 alone may not always be able to provide sufficient effects for the treatment of GBM.
- Inhibiting both EP2 and EP4 might represent a more effective therapeutic strategy for GBM where both receptors are expressed.

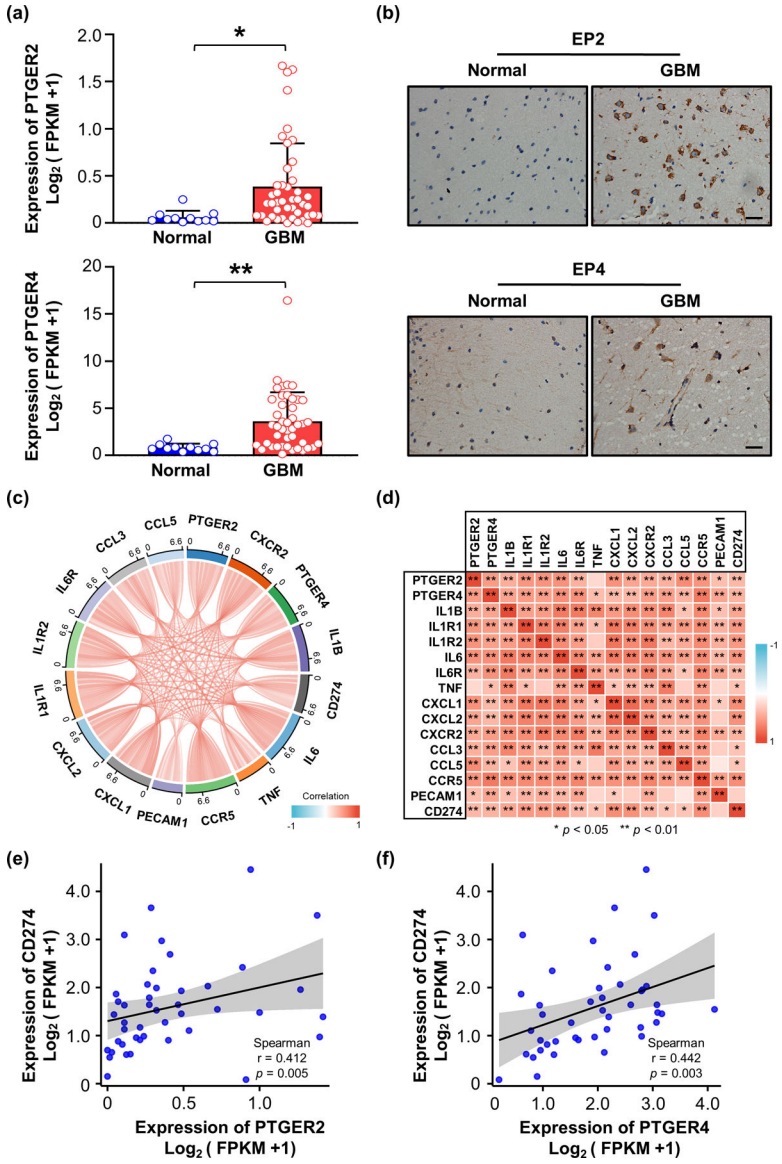

Figure 1. PGE_2 receptors EP2 and EP4 are highly upregulated in human GBMs.

(a) A total of 44 human glioblastoma tissues and 11 control brain tissues were collected and analyzed through RNA sequencing, and the expression levels of EP2 (encoded by *PTGER2*) and EP4 (*PTGER4*) were shown. (*$p < 0.05$, **$p < 0.01$ compared with the normal control group, t test). Data are presented as mean + SEM.

(b) Representative immunohistochemical staining of EP2 and EP4 in human GBM and normal brain tissues. Scale bar = 50 μm.

(c, d) The correlations of EP2 and EP4 with the inflammatory cytokines (IL-6, IL-1β, TNF), chemokines (CXCL1, CXCL2, CCL3 and CCL5) and their corresponding receptors, immune checkpoint PD-L1 (*CD274*) in the GBM tumor tissues. The correlation chord diagram (c) and correlation matrix diagram (d) were presented. ($n = 44$, *$p < 0.05$; **$p < 0.01$, spearman's rank correlation coefficient analysis).

(e) The relationships between EP2/EP4 receptors and PD-L1 in GBM tumor tissues ($n = 44$, spearman's rank correlation coefficient analysis).

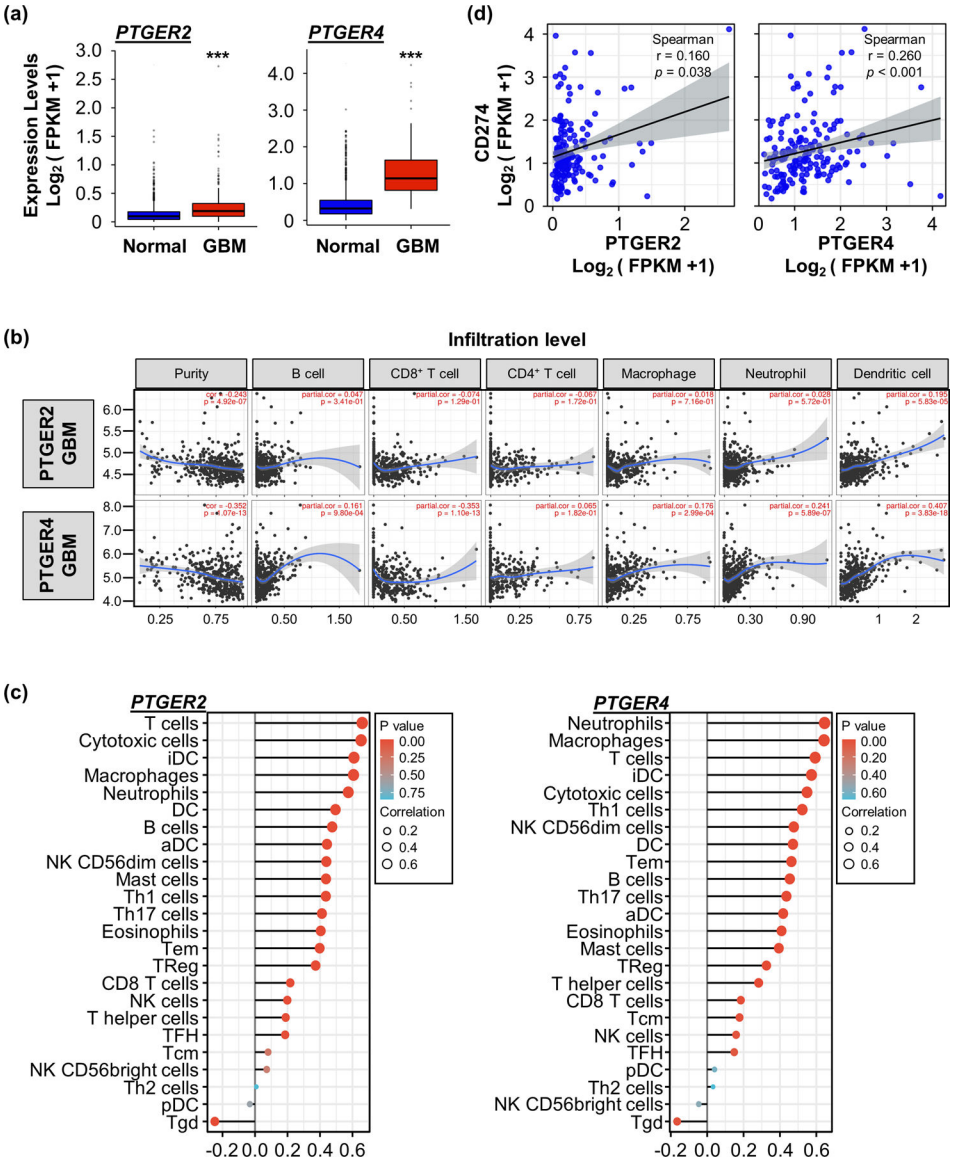

Figure 2. The expression of EP2 and EP4 correlates with tumor-infiltration immune cells in human GBM.

(a) The expression levels of EP2 and EP4 in human GBM tissues from TCGA database (n = 1157 for Normal, n = 166 for GBM, ***$p < 0.001$, Mann-Whitney U test).

(b) Expression correlation between EP2/EP4 and immune cell Infiltration in human GBM were analyzed using TIMER (Tumor IMmune Estimation Resource).

(c) Expression correlation between EP2/EP4 and tumor-Infiltration immune cells in human GBM were analyzed using Immune infiltration algorithm ssGSEA based on the TCGA database.

(d) The spearman correlation analysis reveals that PGE_2 receptors EP2 and EP4 positively correlate with PD-L1 in human glioblastoma from TCGA database (n = 169).

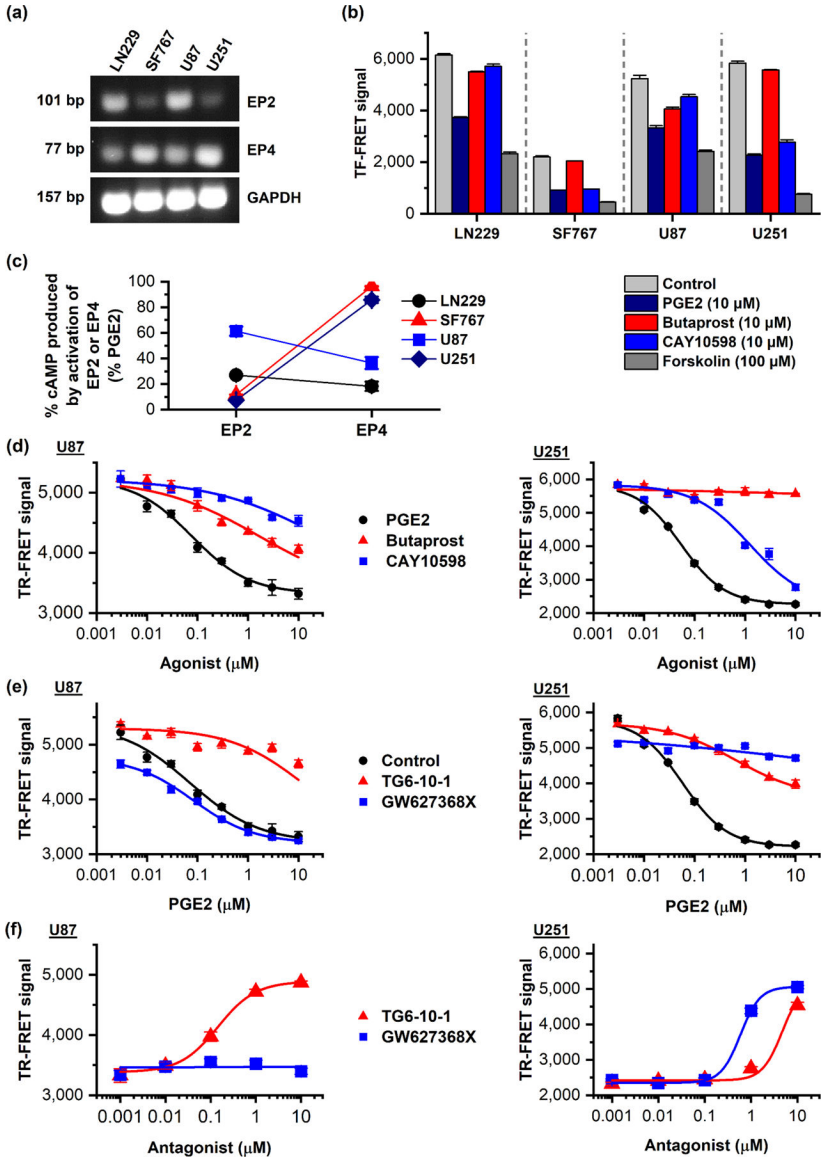

Figure 3. EP2 and EP4 receptors complementarily mediate cAMP signaling in GBM cells.

(**a**) Agarose gel electrophoresis of RT-PCR products of EP2, EP4 and GAPDH in human GBM cell lines: LN229, SF767, U87, and U251.

(**b**) GBM cells were treated with PGE_2 (10 μM), selective EP2 agonist butaprost (10 μM), EP4 agonist CAY10598 (10 μM), or forskolin (100 μM) as positive control. The cAMP signaling in these cells was detected by a time-resolved fluorescence energy transfer (TR-FRET) method, and a lower FRET signal indicates a higher cytosol cAMP level (*$p < 0.05$; **$p < 0.01$; ***$p < 0.001$, compared with the control group, one-way ANOVA and *post hoc* Dunnett's test). Exploratory data are presented as mean + SEM ($n = 4$).

(**c**) The cAMP production via EP2 receptor activation by butaprost and EP4 activation by CAY10598 in GBM cell lines was compared.

(**d**) PGE_2, butaprost, and CAY10598 (0.003 μM, 0.01 μM, 0.03 μM, 0.1 μM, 0.3 μM, 1 μM, 3 μM, 10 μM) induced cAMP synthesis in human GBM cell lines U87 and U251 in

a concentration-dependent manner. The calculated EC_{50}s: 0.08 μM for PGE_2, 1.7 μM for butaprost, and 28 μM for CAY10598 in U87 cells; 0.05 μM for PGE_2, > 1 mM for butaprost, and 1.25 μM for CAY10598 in U251 cells. Exploratory data are presented as mean + SEM (n = 4).

(**e**) EP2 selective antagonist TG6-10-1 (1 μM) and EP4 antagonist GW627368X (1 μM) showed robust inhibition on cAMP production induced by PGE_2 (0.003 μM, 0.01 μM, 0.03 μM, 0.1 μM, 0.3 μM, 1 μM, 3 μM, 10 μM) in human GBM cell lines U87 and U251, respectively. PGE_2 EC_{50}s: 0.07 μM for control, 12 μM for TG6-10-1, and 0.08 μM for GW627368X in U87 cells; 0.06 μM for control, 3.6 μM for TG6-10-1, and 90 μM for GW627368X in U251 cells. Exploratory data are shown as mean ± SEM (n = 4).

(**f**) TG6-10-1 and GW627368X (0.001 μM, 0.01 μM, 0.1 μM, 1 μM, 10 μM) inhibited 1 μM PGE_2-induced cAMP production in human GBM cell lines U87 and U251 in a concentration-dependent manner. IC_{50}s: 0.15 μM for TG6-10-1 and 41 μM for GW627368 in U87 cells; 4.8 μM for TG6-10-1 and 0.6 μM for GW627368X in U87 cells. Exploratory data are shown as mean ± SEM (n = 4).

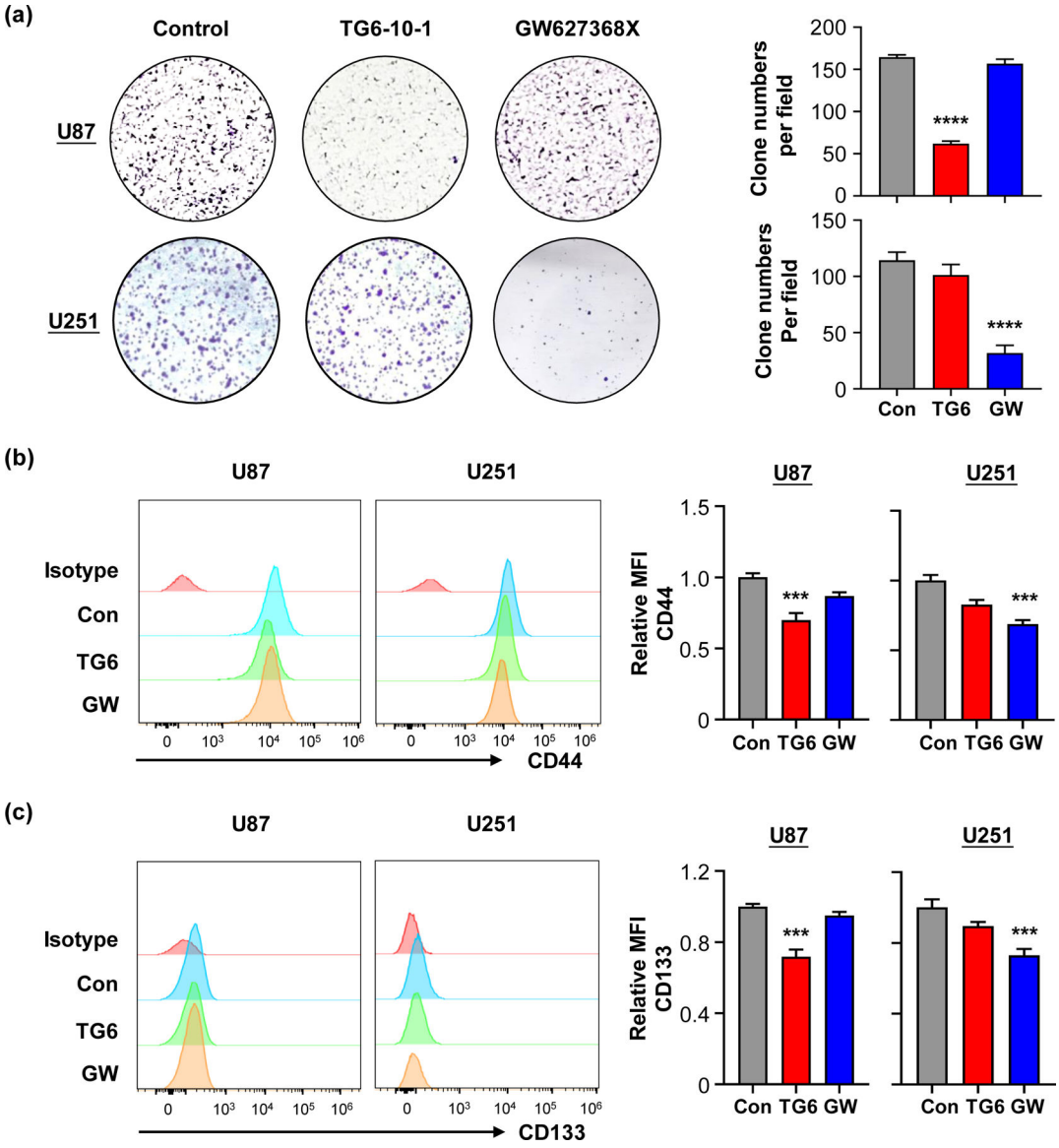

Fugure 4. EP2 and EP4 receptors inhibition diminishs the tumor initiation of GBM cells.

(a) U87 and U251 cells were treated with TG6-10-1 (10 μM) and GW627368X (10 μM) for 7 days, the colonies were stained and visualized with crystal violet dye. ($n = 6$, ****$p <$ 0.0001 vs. corresponding control group, one-way ANOVA and post hoc Dunnett's test for multiple comparisons). Data are presented as mean + SEM. Con, control; TG6, TG6-10-1; GW, GW627368X.

(b, c) Representative flow cytometry plots showing CD44 (b) and CD133 (c) in U87 and U251 cells treated with TG6-10-1 (10 μM) and GW627368X (10 μM) for 48 hours. ($n = 5$, ***$p < 0.001$ vs. corresponding control group, one-way ANOVA and post hoc Dunnett's test for multiple comparisons). Data are presented as mean + SEM.

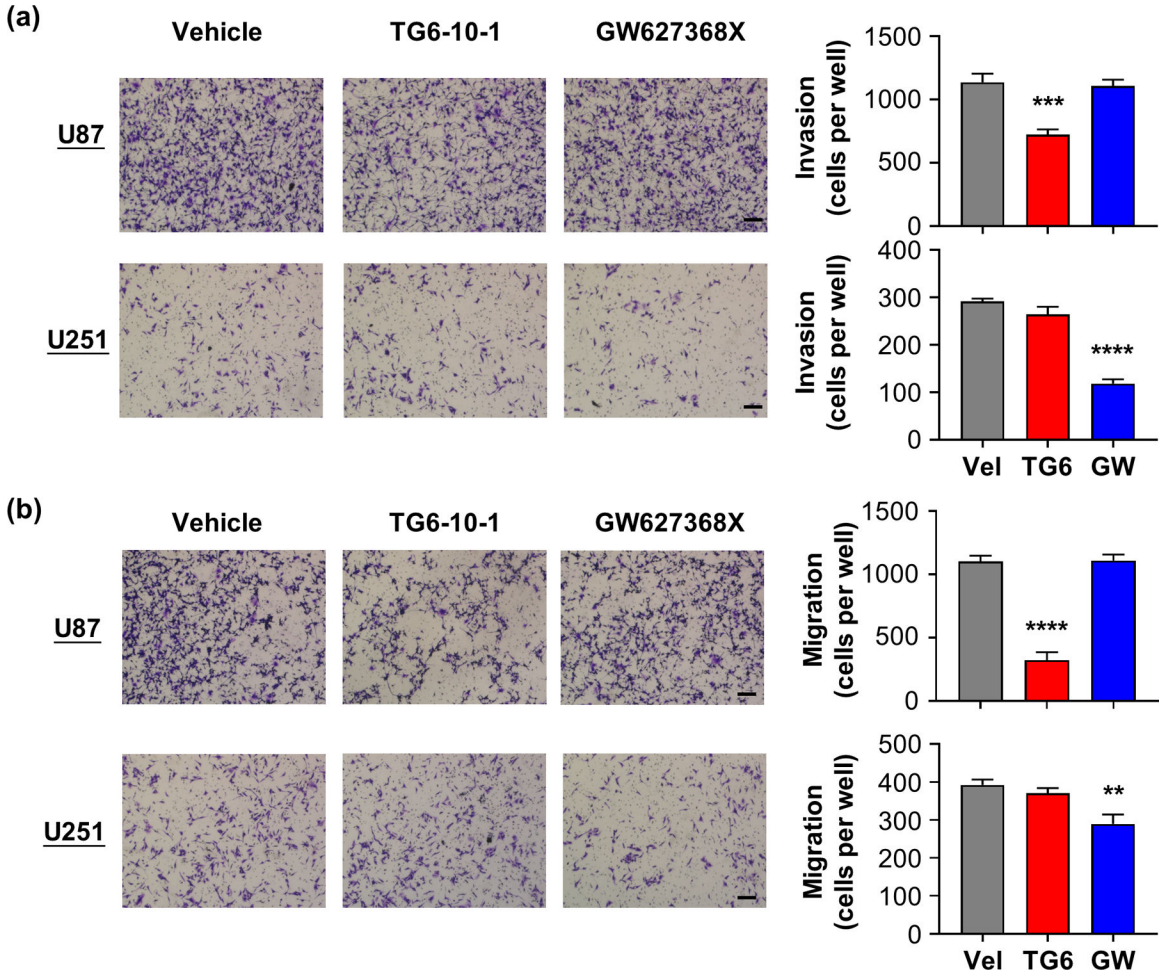

Fugure 5. Inhibition of EP2 and EP4 attenuates the GBM cells invasion and migration.

(a) U87 and U251 cells were seeded into transwell chambers pre-coated with matrigel, followed by treatment with TG6-10-1 (10 μM) and GW627368X (10 μM) for 48 hours. GBM cells passed through the chamber were stained with crystal violet and randomly counted. ($n = 5$, ***$p < 0.001$; ****$p < 0.0001$ vs. corresponding vehicle-treated group, one-way ANOVA and *post hoc* Dunnett's test for multiple comparisons). Data are shown as mean + SEM. Scale bar = 50 μm.

(b) Treating U87 cells with TG6-10-1 (10 μM) and U251 cells with GW627368X (10 μM) for 48 hours attenuated tumor cell migration. ($n = 5$, **$p < 0.01$; ****$p < 0.0001$ vs. corresponding vehicle-treated group, one-way ANOVA and *post hoc* Dunnett's test for multiple comparisons). Data are shown as mean + SEM. Scale bar = 50 μm.

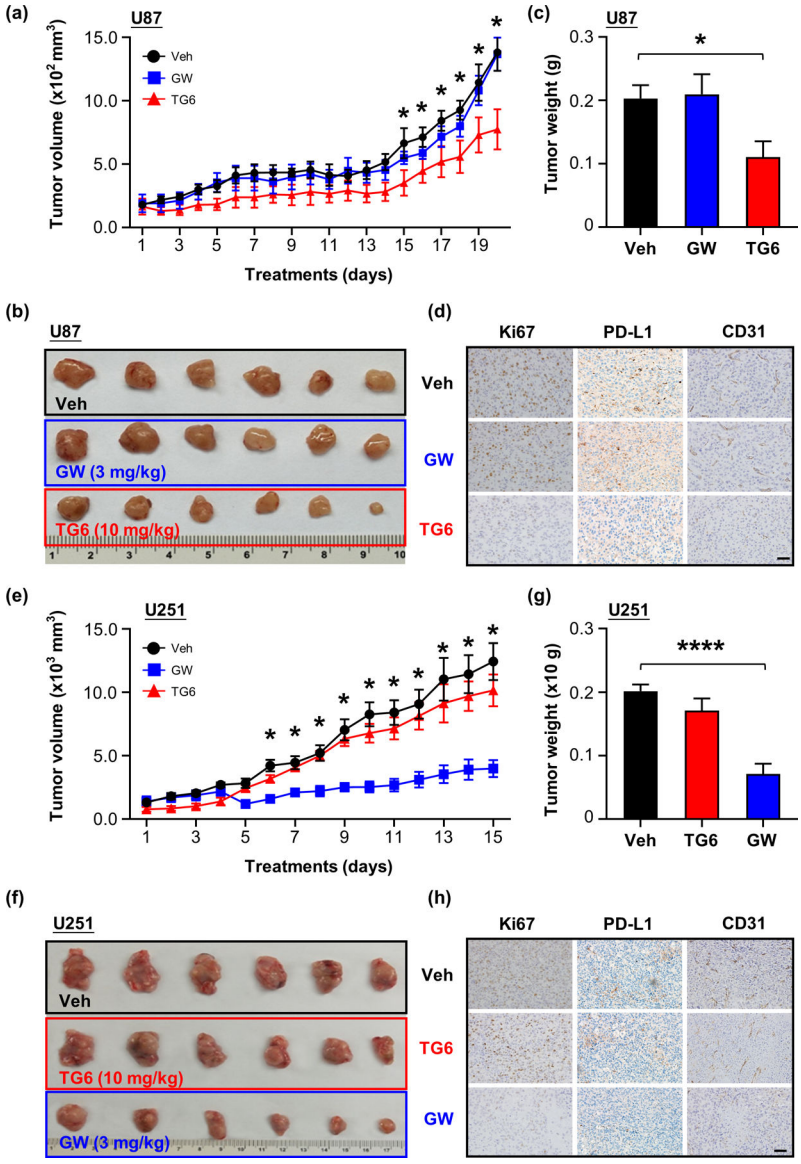

Figure 6. Blockade of EP2 and EP4 receptors impairs the tumor growth *in vivo*.

(a, e) U87 (a) and U251 (e) cells (6×10^6 cells per site) were subcutaneously inoculated into athymic nude mice (female, 4 weeks old). After solid tumors had developed, vehicle (10% PEG 200, 0.5% methylcellulose) or selective EP2 antagonist TG6-10-1 (10 mg·kg^{-1}, p.o, b.i.d) or selective EP4 antagonist GW627368X (3 mg·kg^{-1}, p.o, q.d.) was administered daily for 20 days and 15 days in mice harbored tumors derived from U87 and U251, respectively. Tumor growth was monitored daily by measuring tumor volume using the formula: $V = (\pi/6) \times [(A + B)/2]^3$ (A = longest diameter; B = shortest diameter) ($n = 6$; a: *$p < 0.05$ when compared TG6-10-1 treatment group with vehicle-treated group; e: *$p < 0.05$ when compared GW627368X treatment group with vehicle-treated group; two-way ANOVA and *post hoc* Dunnett's test for multiple comparisons). Data are shown as mean ± SEM. Vel: vehicle; GW: GW627368X; TG6: TG6-10-1.

(b, f) S.c. tumors derived from U87 (b) and U251 (f) after treatments were collected and displayed for comparison.

(c, g) All tumors were weighted and compared between treatment groups ($n = 6$; c: $*p < 0.05$ when compared TG6-10-1 treatment group with the vehicle-treated group; g: $****p < 0.0001$ when compared GW627368X treatment group with the vehicle-treated group; one-way ANOVA and *post hoc* Dunnett's test for multiple comparisons). Data are presented as mean + SEM.

(d, h) IHC staining was performed to detect the expression of Ki67, CD31 and PD-L1 in s.c. tumor tissues derived from U87(d) and U251(h) cells. Scale bar = 50 μm.

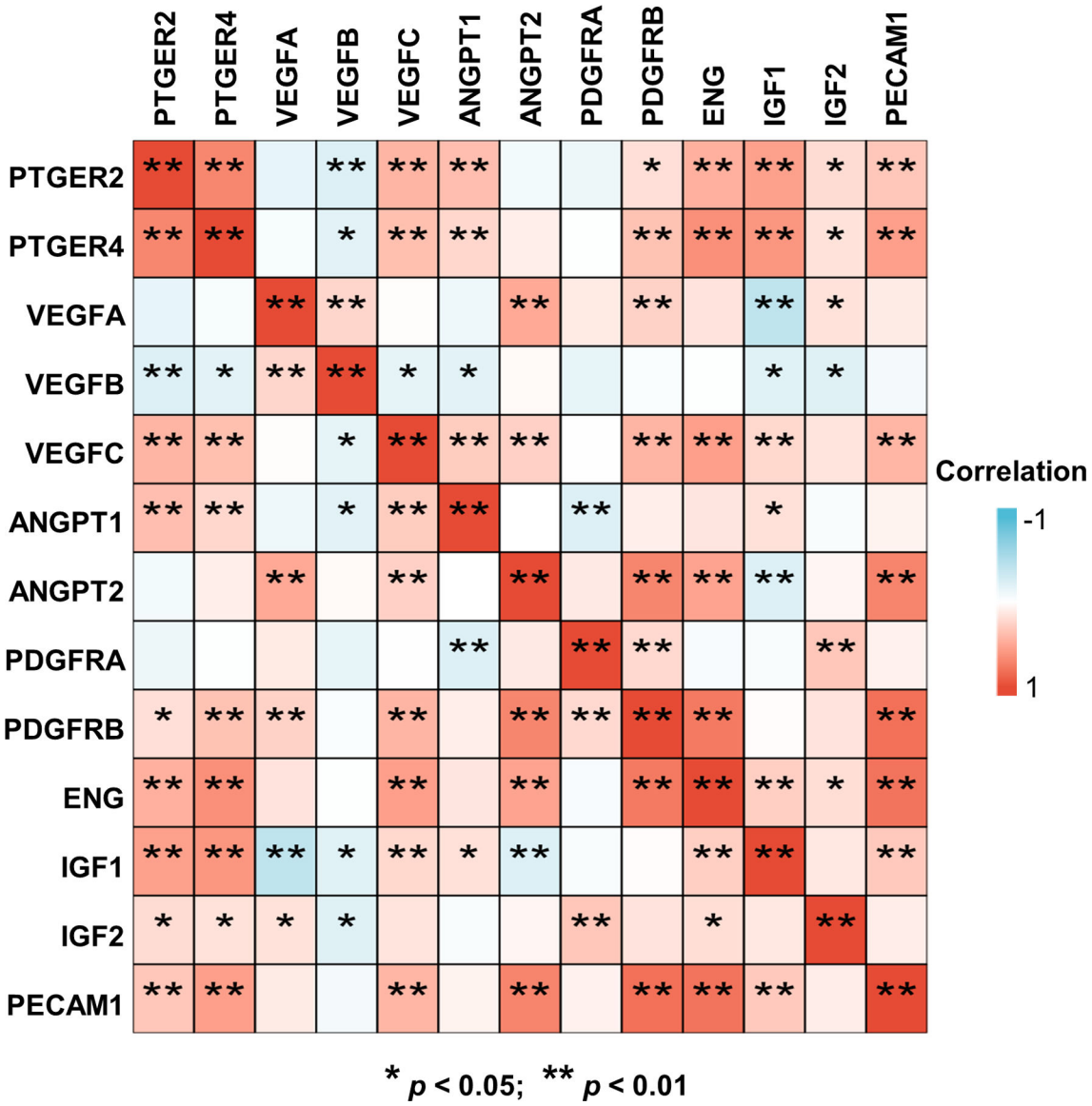

Figure 7. Correlation between angiogenesis-related genes and EP2 and EP4 in human GBM.

The expression relationship between a number of currently known angiogenesis associated genes and prostaglandin receptors EP2 and EP4 was examined by spearman's correlation coefficient analysis using TCGA database (n = 169).

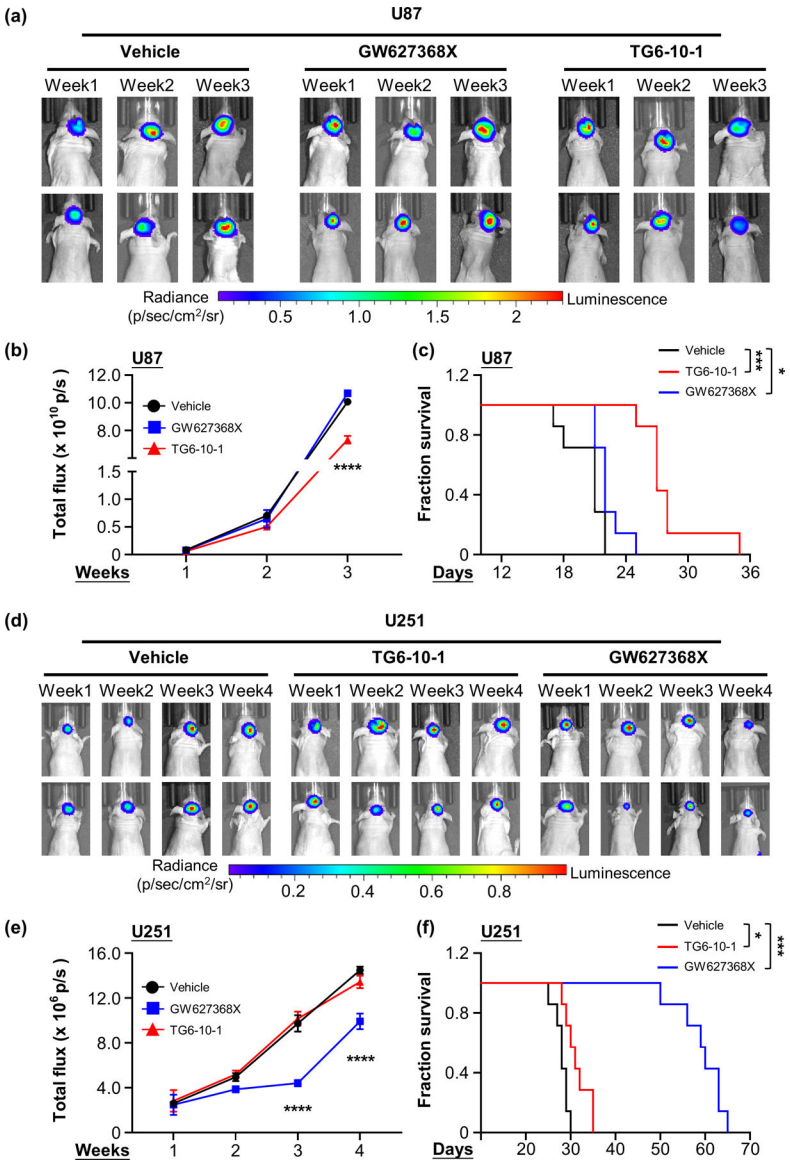

Figure 8. Phamacological inhibition of EP2 and EP4 receptor suppresses the orthotopic glioblastoma growth.

(a, d) Human U87 (a) and U251(d) glioblastoma cells labeled with luciferase were implanted into the right striatum of athymic nude mice (5×10^5 cells per mouse). After recovery from surgery, mice were randomized into three groups ($n = 7$ per group), and administered with vehicle (10% PEG 200, 0.5% methylcellulose) or selective EP2 antagonist TG6-10-1 (10 mg·kg^{-1}, p.o, b.i.d) or selective EP4 antagonist GW627368X (3 mg·kg^{-1}, p.o, q.d.) for 3–4 consecutive weeks. Tumor growth was monitored weekly by bioluminescence using Xenogen IVIS imaging system.

(b, e) Quantification of bioluminescence signals of U87 (b) and U251 (e) to demonstrate the intracranial tumor growth ($n = 5$–7; b: ****$p < 0.0001$ when compared TG6-10-1 treatment group with the vehicle-treated group; e: ****$p < 0.0001$ when compared GW627368X treatment group with the vehicle-treated group; two-way ANOVA and *post hoc* Dunnett's test for multiple comparisons). Data are presented as mean ± SEM.

(c, f) Survival rates of animals that harbored intracranial tumors derived from U87 (c) and U251 (f) cells received vehicle ($n = 7$), TG6-10-1 ($n = 7$) or GW627368X ($n = 7$) for 3 weeks (U87) and 4 weeks (U251). The median survival times of U87 tumor-bearing mice treated by vehicle, GW627368X and TG6-10-1 were 21, 22 and 27 days, respectively. The median survival times of U251 tumor-bearing mice treated by vehicle, TG6-10-1 and GW627368X were 28, 31 and 60 days, respectively. *$p < 0.05$, ***$p < 0.001$, Kaplan-Meier survival analysis with Log-rank (Mantel-Cox) test.